

THE EFFECT OF SHEAR THINNING BEHAVIOUR ON TURBULENT PIPE FLOW

M. RUDMAN AND H. M. BLACKBURN

CSIRO Manufacturing and Infrastructure Technology, Highett Victoria 3190, AUSTRALIA

ABSTRACT

Direct numerical simulation of the weakly turbulent flow of non-Newtonian fluids is undertaken for two different generalised Newtonian rheology models using a spectral element-Fourier method. Results for a power law (shear-thinning) rheology agree well with experimentally determined logarithmic layer correlations and with other previously published experimental work. As the flow index becomes smaller for the same Reynolds number, the flow deviates further from the Newtonian profile and the results suggest that transition is delayed. Predicted friction factors fall above those in the literature, but below the Newtonian values indicating that shear thinning behaviour alone can result in drag reduction. Results for a Herschel-Bulkley model (yield stress + shear-thinning) are compared to corresponding experimental measurements and found to be in good agreement. Use of this DNS technique shows great promise in understanding transition and turbulence in non-Newtonian fluids.

NOMENCLATURE

D	Pipe diameter
f	Fanning friction factor
K	Fluid consistency
n	Flow index
r	radius
P_{rz}	Turbulence production
Re_g	Generalised Reynolds number (Eqn 4)
Re_{MR}	Metzner-Read Reynolds number (Eqn 5)
R_{ww}	Two-point velocity correlation
U_C	Centreline axial velocity
U^+	Scaled velocity (usual log scaling)
\hat{U}	Scaled velocity (see Eqn 7)
U_τ	Friction velocity
U_r	Radial velocity
V_θ	Azimuthal velocity
W_z	Axial velocity
y^+	Scaled distance from pipe wall (usual log scaling)
\hat{y}	Scaled distance from pipe wall (see Eqn 7)
$\dot{\gamma}$	Shear rate
η	Dynamic viscosity
η_w	Mean pipe wall viscosity
τ_w	Mean pipe wall shear stress
τ_Y	Fluid yield stress

INTRODUCTION

The flow of non-Newtonian fluids and slurries in pipes occurs in a wide range of practical applications in the process industries. If the fluid has a significant yield stress, or if its effective viscosity is high, industrially relevant flow rates may occur in the laminar flow regime (e.g. thickened slurry discharge in the minerals industry). However in some cases the flow can be turbulent and there are advantages in operating pipe flows in a

transitional flow regime because the specific energy consumption is lowest there. In the case of solids transport, the flow structures associated with intermittency may be used to keep particles in suspension without the much higher pressure losses of the fully turbulent regime. Although some experimental work has appeared on the transitional and turbulent flow of non-Newtonian fluids ([8], [9], [13]), little fundamental understanding exists. General theories of turbulence are lacking for non-Newtonian fluids, and the development of mathematical and computational models is not well advanced.

Computational modelling of non-Newtonian flows, especially using direct numerical simulation (DNS), shows promise in helping to understand transition and turbulence in these fluids. There have been some DNS of the turbulent flow of polymer solutions with the aim of understanding the causes of drag reduction (e.g. [1], [4], [19]). In those studies, dilute polymer solutions were considered in which shear thinning behaviour was negligible and elongational (visco-elastic) effects were taken into account using various methods for the extra elastic stresses. However, for a wide range of important materials, the non-Newtonian rheology is primarily of a shear-thinning nature. Malin [12] considered turbulent pipe flow of power law fluids using a Reynolds-averaged approach and a modified k - ϵ model. Reasonable agreement with experimental data was obtained after modifying the wall damping functions, however this approach is at least in part empirical, and does not shed light on the fundamental flow effects arising from shear thinning behaviour. Apart from some recent work ([14], [15]) there have been few published CFD investigations of turbulent flows of shear-thinning non-Newtonian fluids without visco-elasticity.

Experimental results show that compared to Newtonian fluids, the transition to turbulence may be delayed in shear thinning fluids, ([13], [15]) (i.e. it occurs at a higher generalised Reynolds number). There is also evidence that the radial and azimuthal turbulence intensities are lower by 20–40% for a power law fluid compared to a Newtonian fluid, whereas the axial intensities may be marginally higher ([8], [9], [13]). The aim of the present study is to investigate the effect of rheological parameters and to consider the modification to the flow that arises in the presence of a fluid yield stress.

Rheology Models

This paper describes a study undertaken of shear-thinning non-Newtonian fluids whose rheology is described by a generalised Newtonian model, i.e. one in which an isotropic viscosity dependant on flow properties is applicable. In the present work, particular fluids are considered in which the viscosity η can be described using either the power law (Ostwald-de Waele) model

$$\eta = K\dot{\gamma}^{n-1} \quad (1)$$

or the Herschel–Bulkley model

$$\eta = \frac{\tau_y}{\dot{\gamma}} + K\dot{\gamma}^{n-1} \quad (2)$$

where $\dot{\gamma}$ is the shear rate, K is the consistency, n is the flow index, and (in the case of the Herschel–Bulkley model) τ_y is the yield stress. In the case of the power-law model, $n < 1$ for shear-thinning, $n = 1$ for Newtonian, and $n > 1$ for shear-thickening fluids. The shear rate is estimated as the second invariant of the rate of strain tensor, S .

Generalised Reynolds number

When the viscosity varies in space and time, the appropriate viscosity scale to use in order to define a Reynolds number is not obvious. There are a number of possible choices and that used here is the mean wall viscosity, η_w , that can be determined *a priori* from the mean wall shear stress, τ_w , that in turn is equal to $D/4$ times the pressure gradient.

Assuming a Herschel–Bulkley model it is easy to show that the mean wall viscosity is given by

$$\eta_w = \frac{K^{1/n} \tau_w}{(\tau_w - \tau_y)} \quad (3)$$

For the power law model, τ_y is set to zero in Eqn. . The resulting generalised Reynolds number

$$\text{Re}_g = \frac{\rho \bar{U} D}{\eta_w} \quad (4)$$

The generalised Reynolds number used here is different to the more traditional Metzner–Reed Reynolds number that, for a power law fluid, can be written in closed form as

$$\text{Re}_{MR} = \frac{8\rho \bar{U}^{2-n} D^n}{K(6 + 2/n)^n} \quad (5)$$

(For fluids other than power law fluids, a Metzner–Reed Reynolds number can also be calculated, see [7].)

The generalised Reynolds number, Re_g , reflects flow behaviour in the near wall region that plays a fundamental role in transition and the development of turbulence in wall bounded flows of Newtonian fluids. As such, it is believed that this is a suitable basis on which to compare and order simulation results.

NUMERICAL METHOD

The spatial discretisation employs a spectral element–Fourier formulation, which allows arbitrary geometry in the (x, y) plane, but assumes periodicity in the z (axial, or out-of-plane) direction. Details of the numerical method may be found in [2], [10], [11] and are not repeated here in the interests of space.

Because both the power law and Herschel–Bulkley rheology models have a singular viscosity at zero shear rate, a ‘cut-off’ value is used, below which the shear rate is assumed to be constant when computing the viscosity. The cut-off value is chosen to be 10^{-5} times the mean shear rate and is not observed to cause any stability problems or significant errors. The cut-off is almost never invoked in practice for either the power law or Herschel–Bulkley simulations because the calculated shear rates throughout the flow (even in the less active core regions) are nearly always several orders of magnitude above the cut-off value.

The computations reported here were carried out using 16, 32 or 64 processors on the Australian Partnership for Advanced Computing (APAC) cluster. Run times were

typically in the order of 1000 CPU hours to reach a statistically steady state, with an additional 500–1000 CPU hours used to obtain statistics. These latter times corresponded to 30–60 fluid transit times over the length of the computational domain.

Validation and grid refinement

The underlying numerical code has been validated for both DNS and LES of pipe and channel flow ([2], [16], [17]). The implementation of the power-law non-Newtonian viscosity was validated against laminar pipe flow and axisymmetric Taylor–Couette flow of power-law fluids, both of which have analytic solutions. For the Herschel–Bulkley model, validation was against laminar pipe flow only. In all cases, numerical and theoretical velocity profiles agreed to within 0.01% and the code is believed to be accurately predicting the flow of non-Newtonian fluids with generalised Newtonian rheologies. To check the grid convergence of the solutions, one simulation (with $n=0.69$) was run at three different resolutions. A coarse resolution given by 80 Fourier modes (i.e. 160 z -planes) and 105 6×6 elements, a medium resolution (at which the simulations reported here are undertaken) of 108 Fourier modes and 105 8×8 elements and a fine mesh with 192 Fourier modes and 189 8×8 elements. The mean velocity profiles were almost indistinguishable from each other. The turbulence intensities and Reynolds stresses are shown in **Figure 1**. Clearly, the results for the coarse mesh lie approximately 5% below the other results for the turbulence intensities, although agree well for Reynolds stress. The difference between the medium and fine mesh results are insignificant, justifying the use of the medium size mesh for the simulations reported here.

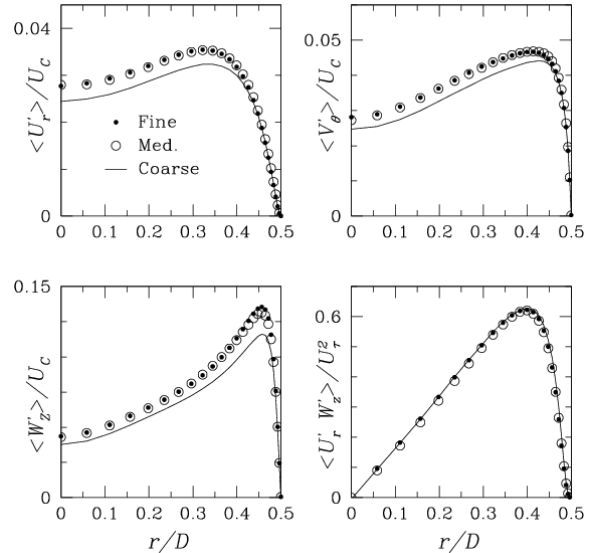


Figure 1: Turbulence intensities and Reynolds stresses for simulations undertaken at fine, medium and coarse resolutions. The difference between the medium and fine results is insignificant.

Computational Parameters

The computational domain consists of 105 8th-order elements in the pipe cross section (see [14]) and 80–128 Fourier modes (i.e. 160–256 data planes) in the axial direction, with domain lengths of $4\text{--}5 \pi D$ depending on Reynolds number and flow index.

Wall units are introduced in a similar manner to the Newtonian analysis with the wall viscosity taking the place of the Newtonian viscosity. Hence the friction velocity is defined as $U_\tau = \sqrt{\tau_w/\rho}$, the non-dimensional velocity is $U^+ = U/U_\tau$ and the non-dimensional distance from the wall is written $y^+ = (\rho U_\tau / \eta_w) y$. In terms of these wall units, the

near-wall mesh spacing is $r^+ \approx 0.5$, $R\theta^+ \approx 8$ and $z^+ \approx 35$. This resolution is perhaps marginal in the streamwise direction, although a grid convergence study discussed above suggests that significantly increasing the streamwise resolution had little effect on the turbulence statistics, and is therefore sufficient for this investigation.

In order to maintain a uniform generalised Reynolds number in the power law simulations, as n was changed both the consistency, K , and the driving pressure gradient were altered to maintain the same wall viscosity and superficial velocity. A similar process was used in the Herschel-Bulkley simulations while the yield stress was kept constant.

RESULTS

Mean Flow Profiles for Power Law Fluids

The mean axial velocity for the three simulations at $Re_g=5500$ for $n=0.5$, 0.69 and 0.75 are shown in **Figure 2** and **Figure 3** and compared to a Newtonian profile at the same Reynolds number. As the flow index n increases, the profiles for the power law fluids approach the Newtonian profile, as expected. The results for $n=0.5$ fall sufficiently above the Newtonian profile suggesting that this flow is transitional – this point will be discussed in more detail below.

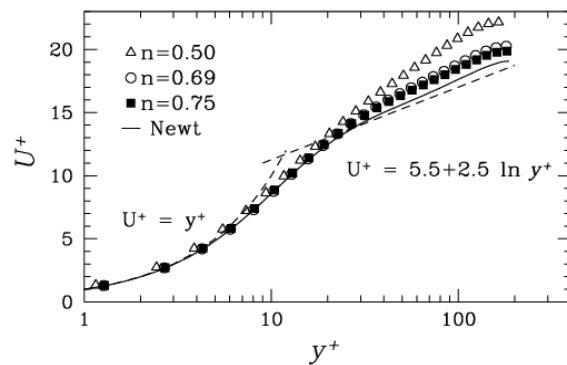


Figure 2: Velocity profiles for the turbulent flow of three power law fluids at $Re_g=5500$ ($n=0.5$, 0.69 and 0.75) non-dimensionalised using the conventional non-dimensionalisation with the wall viscosity taking the place of the Newtonian viscosity. Shown for comparison is a correlation for low Reynolds number turbulent pipe flow (dashed line) and DNS results at $Re=5500$ (solid line), both for a Newtonian fluid.

In [3], Clapp reports the results of experimental measurements of the turbulent pipe flow of power law fluids with flow indices in the range $0.698-0.813$. Based on these measurements, dimensional arguments, and early measurements of turbulent Newtonian pipe flow reported in [5], Clapp determines that the logarithmic velocity profile for the turbulent flow of power law fluids is a function of the flow index, n , and satisfies

$$\hat{U} = \frac{A}{n} + \frac{B}{n} \ln \hat{y} \quad (6)$$

where

$$\hat{y} = [(\rho \tau_w^{2-n})^{1/2} / K] y^n \quad (7)$$

and $\hat{U} = U^+$. The values of the parameters in Eqn. (6) given by Clapp are $A=3.8$ and $B=2.78$, and were chosen to give collapse to the experimental measurements of turbulent pipe flow of a Newtonian fluid ($n=1$) reported in [5]. The values of these coefficients for well developed turbulent flow of Newtonian fluids are now generally accepted to be $A=5.0$, $B=2.5$ (while for low Reynolds number flow, $A=5.5$ gives a closer fit to the data) [6]. Thus it may be expected that $A=5.5$, $B=2.5$ should be used.

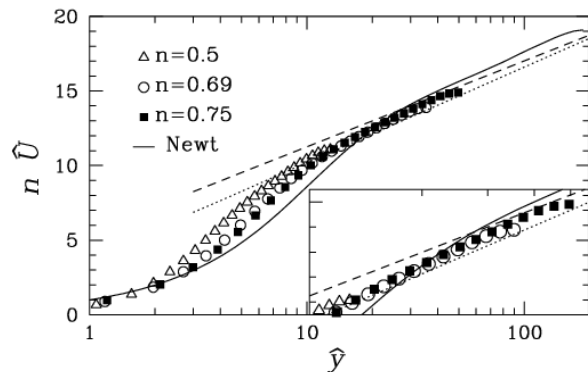


Figure 3: As in **Figure 2**, but plotted using Clapp's non-dimensionalisation. The dotted line is Clapp's correlation using his coefficients (3.8, 2.78) and the dashed line is using the generally accepted values of (5.5, 2.5) for low Reynolds number Newtonian flow.

In **Figure 3** the mean axial velocity (multiplied by n) is compared to Clapp's correlation. The dotted line is the logarithmic profile using the coefficients $A=3.8$, $B=2.78$ and the dashed line uses $A=5.5$, $B=2.5$. Clearly seen in this figure is that the CFD results for all three flow indices collapse to a similar profile and agree quite well with the general form of Clapp's correlation – they fall between the dotted and dashed lines for $\hat{y} > 10$. Although Clapp's correlation has drawbacks (in particular the velocity gradient predicted at the pipe centre is non-zero) and other correlations exist that include better approximations for the turbulent core [18], it is only strictly applicable in the logarithmic region and has the benefit that it is easy to calculate. The results here suggest that it is applicable, and perhaps for a wider range of flow indices than Clapp's experiments, although Clapp's original coefficients probably need to be modified in light of more recent turbulence measurements in Newtonian fluids.

Turbulence intensities, turbulence production, Reynolds shear stresses and r.m.s. streamwise vorticity fluctuations are plotted in **Figure 4**. For both the axial turbulence intensities and the Reynolds stresses, the results for the power law fluids are close to the Newtonian results (DNS at $Re=5500$). However for both radial and azimuthal velocity fluctuations, the values for the power law fluids are significantly lower than the Newtonian case. This behaviour has been observed experimentally ([9], [13]) in turbulent flow of non-Newtonian fluids, although currently there is no clear understanding of why this is the case.

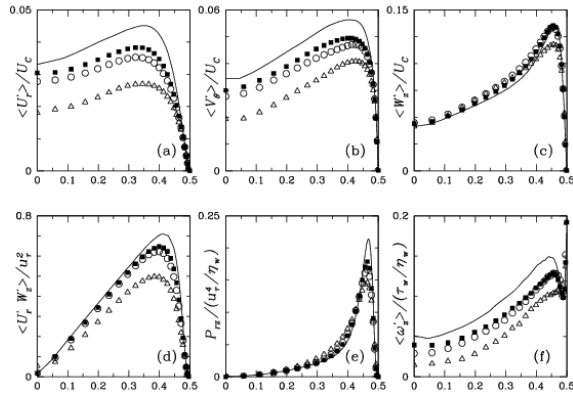


Figure 4: Turbulence intensities as a function of r/D (a) radial, (b) azimuthal and (c) axial, (d) turbulence production, (e) Reynolds shear stress, and (f) r.m.s. axial vorticity fluctuation. (Solid line for Newtonian DNS, power law fluids are $n=0.5$ (Δ), $n=0.69$ (\circ) and $n=0.75$ (\blacksquare))

Similar behaviour is also found in measurements of low Reynolds number Newtonian turbulence. Low and high Reynolds number flows produce almost identical (non-dimensionalised) axial velocity fluctuations, whereas the transverse components are weaker for low Reynolds number and have their peak somewhat closer to the pipe wall [6]. Thus these phenomena in the shear thinning results here are possibly features of flows that are not fully developed and in which a self-similar velocity profile is not yet established in the pipe.

Because the viscosity is higher in the core region (in the shear thinning case), the turbulence is not as fully developed there, especially for the fairly low generalised Reynolds number of 5500 used in the simulations here. Consequently, lower transverse fluctuations might be expected in shear thinning fluids in the core region simply because of this. The results in [15] suggest that as Re_g increases, the transverse velocity fluctuations do increase, although it is not clear if the gap between them and the Newtonian curve will be breached or not. It appears possible that the increased viscosity in the core regions of the flow in shear thinning fluids may always result in lower fluctuations than in a Newtonian fluid, although conclusive evidence must await further work. As n approaches unity in **Figure 4**, the non-Newtonian results all approach the Newtonian correlations, as expected.

The distance from the wall of the peak velocity fluctuations and Reynolds stress generally increases as the flow index decreases, indicating an thicker buffer region for more shear thinning fluids. The exception is for the case of $n=0.5$ that is related to the transitional nature of this flow as discussed in more detail in a later section. The production of turbulence is given by

$$P_{rz} = U_r' W_z' \frac{\partial \overline{W}}{\partial r} \quad (8)$$

and is plotted in **Figure 4e**. As seen, the maximum production occurs at a value of $y^+=10$ for the Newtonian fluid. For the power law fluids this distance increases slightly for $n=0.75$ and 0.69 , decreasing slightly for $n=0.5$. The r.m.s fluctuation of the streamwise vorticity is plotted in **Figure 4f** and shows slightly lower peak values as n

decreases, with the peak occurring slightly closer to the wall than in the Newtonian case.

The mean wall streak spacing for the simulations was determined from the azimuthal two-point correlation of the fluctuating axial velocity and is shown in **Figure 5** (the correlation is defined as $R_{ww} = \langle W'(\theta)W'(\theta + \delta\theta) \rangle$).

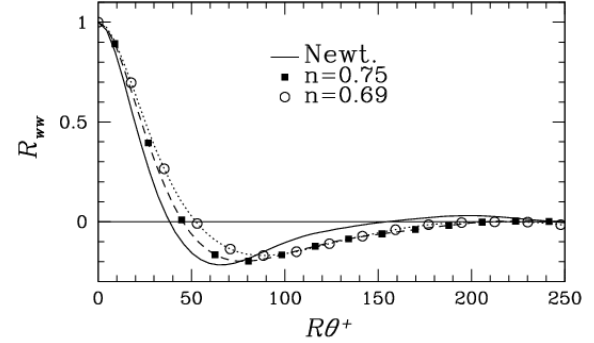


Figure 5: Azimuthal two-point correlation of the fluctuation velocity) at $y^+=20$. The mean streak spacing is estimated as twice the value of separation at the minimum value of R_{ww} .

As seen, the streak spacing for the Newtonian simulation is approximately 125 wall units, for $n=0.75$ it is 155 wall units and for $n=0.69$ it is 180 wall units. This is consistent with the observation that the maximum radial and azimuthal velocity fluctuations occur slightly further from the wall. It was not possible to estimate a meaningful streak spacing for $n=0.5$.

It is interesting to compare the shear thinning results here to those for viscoelastic fluids presented in [1], [4], [19]. In those studies, the conclusion was drawn that polymer additives modify the turbulent structure in the buffer layer ($10 < y^+ < 30$) to increase the stream-wise vortex size, lessen the stream-wise vortex strength, and consequently supply less energy to the log layer. The reduction in advective transport of high-momentum fluid from the core toward the wall ultimately leads to the prediction of drag reduction. Correlated to the weaker vortices were reduced wall normal and span-wise velocity fluctuations compared to the Newtonian case (these correspond to radial and azimuthal fluctuations here). It was also observed that stream-wise (axial) fluctuations were slightly higher than the Newtonian case. As the degree of visco-elasticity increased, these trends increased and it was seen that the mean velocity log layer slope increased also.

The majority of these phenomena are similar in character to those observed here when “degree of viscoelasticity” is replaced by “degree of shear thinning”. Recall that these results are for a fluid that is purely shear thinning. A final comment regarding **Figure 4** is that the similarity in shape and the location of maxima between the shear thinning fluids and the Newtonian case provide evidence that non-dimensionalisation based on the mean wall viscosity, η_w , and hence use of Re_g , is a reasonable basis on which to compare results.

Friction factors

The Fanning friction factor, f , is defined as the non-dimensional wall shear stress and is defined as

$$f = \tau_w / \rho \overline{U}^2 \quad (9)$$

For shear thinning fluids, the friction factor is traditionally plotted against the Metzner-Reed Reynolds number

(Eqn. (5)). The results obtained numerically here are compared to the friction factors determined by Dodge and Metzner [7] in **Figure 6**.

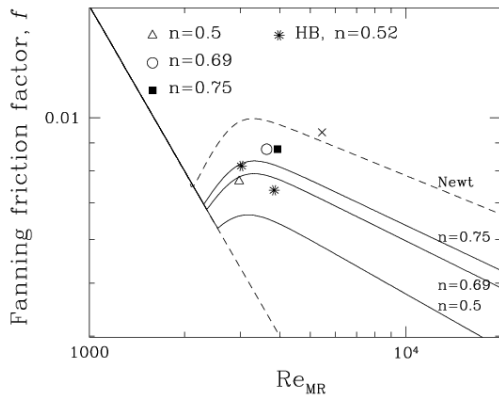


Figure 6: Fanning friction factors determined for the CFD simulations as a function of the Metzner-Reed Reynolds number. The Herschel-Bulkey results are denoted with a star and the cross is from DNS results of a Newtonian fluid at $Re=5500$.

The numerical results predict friction factors that are lower than the corresponding values for a Newtonian fluid. Qualitatively they agree with experimental observations [7] in which shear thinning behaviour was seen to lead to a reduction in friction factor for a fixed Re_{MR} . Quantitatively, it is clear that the predicted values from simulation are higher than those measured in [7] by approximately 10-15% – the reason for this difference is unclear. It is possible that insufficient domain length in the simulation might be affecting the results. It may also be possible that the model fluids in [7] were not sufficiently well characterised as a power law fluid over the range of shear rates that occurred in the experiments, however it is difficult to know if this is the case.

Intermittency and Transition for Power Law Fluids

Time traces of velocity and pressure signals for $n=0.5$ and 0.75 are shown in **Figure 7** (traces at the centreline (dashed line) and near wall (solid line) are shown, although are difficult to distinguish except for the case of the axial velocity component, W). There is a clear distinction between the results for the two different flow indices. The signals for $n=0.75$ (lower three graphs) appear as a fairly random perturbation around a mean value, whereas the signals for $n=0.5$ (upper three graphs) are clearly showing large scale coherent excursions with a random signal superimposed on top. The period of these large deviations is found to be approximately equal to the length of the computational domain ($5\pi D$) divided by the centreline velocity – hence the results are a computational artefact and cannot be relied on as an accurate representation of the real flow for the case of $n=0.5$. The axial extent of these structures is significantly less than the domain length (approximately half, see contours of the axial velocity near the pipe wall in **Figure 8**) yet they are self-sustaining over many transit times of the domain. This result suggests that the flow is likely to be transitional and in reality will contain intermittent phenomena.

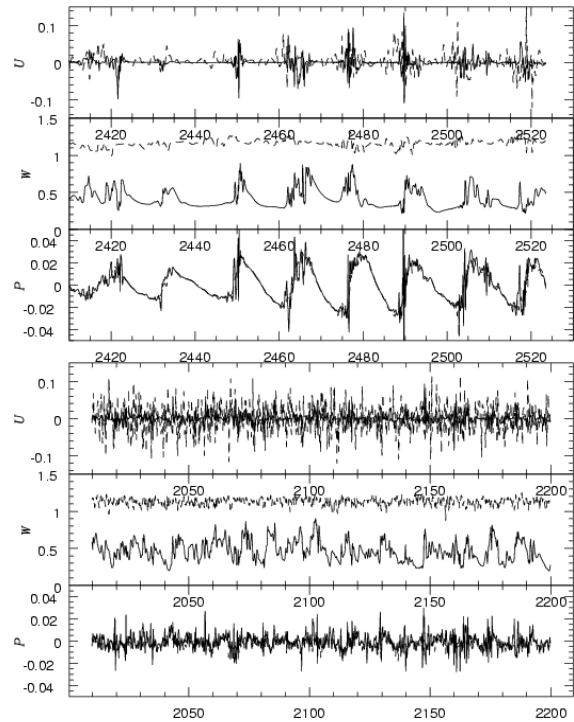


Figure 7: CFD predicted wall-normal velocity, axial velocity and pressure signals near the wall (solid line) and near pipe centre (dashed line) for $n=0.5$ (top three graphs) and $n=0.75$ (bottom three graphs). (All units are non-dimensionalised.)

Figure 8 shows that for the case of $n=0.5$ (top panel), a large region of turbulent activity exists toward the left of the domain whereas the region near the centre of the flow is fairly devoid of unsteady structure.

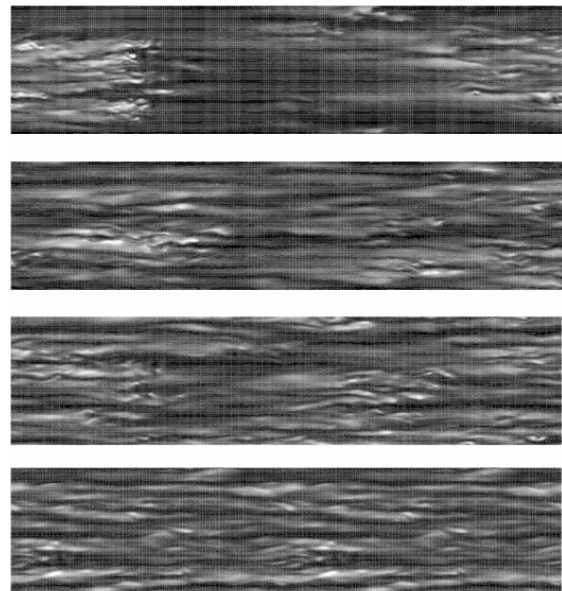


Figure 8: Predicted axial velocity close to the pipe wall for power law fluids, $Re_g=5500$, $n=0.5$ (top), 0.69 , 0.75 and Newtonian fluid ($Re=5500$) (bottom). (The pipe surface has been rolled flat and the flow is from left to right. White represents high velocity and black low.)

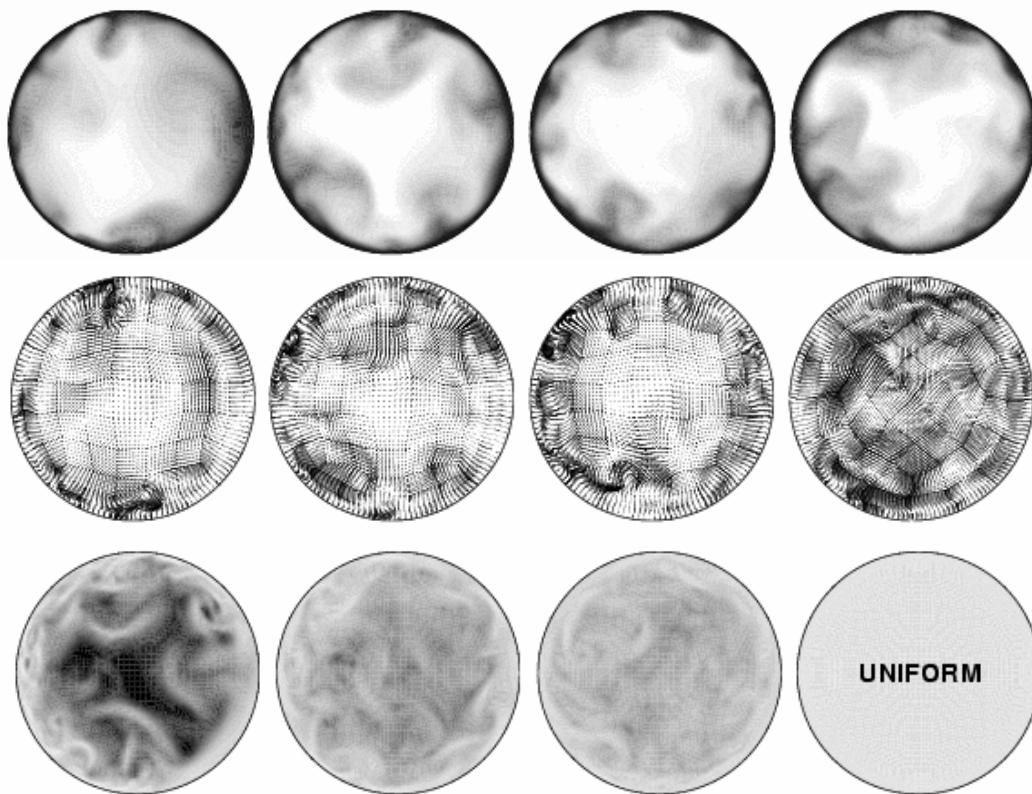


Figure 9: Instantaneous contours of axial velocity, in-plane velocity vectors, and viscosity for power law fluids, $Re_g=5500$ and $n=0.5$ (left), 0.69, 0.75 and Newtonian fluid ($Re=5500$) (right). (For axial velocity, white contours are high and black low. For viscosity, white is low viscosity and black high.)

This type of flow shows typical transitional behaviour and is similar to the turbulent puffs observed in Newtonian fluids in the transitional regime, although it occurs here at a generalised Reynolds number that is quite high compared to Newtonian transition. In the simulation, the active region of the flow continually moves along the pipe and appears to preferentially occur on one side so that the average velocity profile over approximately ten domain transit times (100 pipe diameters) shows some asymmetry. This suggests that permanent asymmetry might be able to be sustained in the transitional regime for power law fluids if a preferential mechanism exists for triggering the puffs (for example an upstream pipe bend), and may explain the asymmetry observed in experiments in [9]. Because of the short domain, this possibility is purely speculative although it warrants a more detailed study. The $n=0.5$ is being re-run with a domain length that is twice as long, although results are not currently available for comparison. As the flow index increases, the distribution of wall streaks becomes more homogeneous in **Figure 8**, although there are still local structures for both $n=0.69$ and $n=0.75$. In each case, the wall streaks are quite long, further evidence that the flow is not fully developed for any of the three power law fluids at this Re_g . However the time series for $n=0.69$ and 0.75 do not show large scale time coherence, indicating that these flows are of a fundamentally different character to the case of $n=0.5$ which can be categorised as transitional. For the case of $n=1$ (a Newtonian fluid) the structure is more random and the streaks shorter, indicative of more

developed turbulence. These results taken together are evidence that transition is delayed for more shear thinning fluids using the assumption that Re_g is a valid basis for comparing them.

Instantaneous snapshots of cross-sectional velocities, contours of axial velocity and contours of viscosity for $Re_g=5500$ are shown in **Figure 9**. These cross sections are taken at an axial location that is just upstream (to the left) of the intense turbulent structure for $n=0.5$ in **Figure 8** and highlight the most unsteady regions in the pipe. The contour scales are identical for each flow index and the magnitude of the cross sectional velocity scales are also equal. They show the degree of unsteadiness in the flow as well as the degree to which the major unsteady structures are confined to regions close to the pipe wall for the power law fluids, whereas there is a significantly increased degree of structure in the core region of the Newtonian fluid.

Clearly seen are the lower viscosities (indicative of higher shear rates) in the wall regions in the power law plots of viscosity. A plot of the mean viscosity as a function of radius for the three power law simulations is given in **Figure 10**. Of note is the range of viscosities, with a relatively small difference in mean viscosity between wall and centreline for $n=0.75$ (a factor of approximately 2), whereas a factor of approximately 5.4 applies for $n=0.5$. This difference is also seen in the instantaneous viscosity plots in **Figure 9** where the higher viscosities (seen as dark contours) are quite prominent.

This behaviour is expected because for more shear thinning fluids, with the same value of mean wall-viscosity, higher core viscosities are inevitable. The mean

viscosity averaged over the domain for the three power law cases is 1.49, 1.86 and 3.35 times the wall viscosity for $n=0.75$, 0.69 and 0.5 respectively.

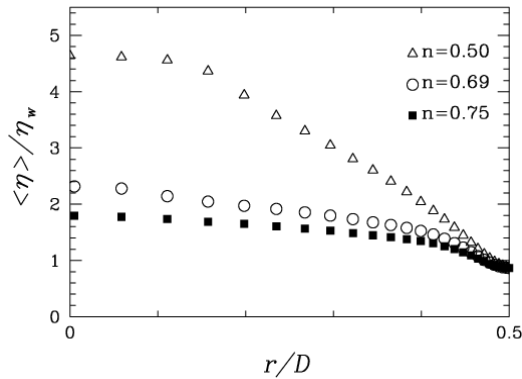


Figure 10: Mean normalised viscosity as a function of radius for power law fluids at $Re_g=5500$.

Results for the Herschel–Bulkley Fluid

Results for the Herschel–Bulkley fluid are preliminary and two simulations have been run for one fluid rheology (0.05 wt% Ultrez 10 solution) with a yield stress of $\tau_y=1.35$ Pa, a consistency $K=1.203$ and a flow index $n=0.52$. The experimental measurements indicated that a pressure gradient of 1.42 kPa/m resulted in a superficial velocity of 3.36 m/s in the line (I.D. of 105 mm) and a generalised Reynolds number of $Re_g=7027$.

When the same values as the experiment are used in the simulation, the superficial velocity predicted by the simulation is 11% lower than the measured value and the predicted Re_g is 5662 (the discrepancy is larger than 11% because the mean wall viscosity is also different). A second simulation was run at a higher pressure gradient (1.75 kPa/m) and resulted in a superficial velocity of 3.5 m/s and $Re_g=8130$. The two simulations bracketed the Re_g of the experimental measurements. The discrepancy between CFD and measurement is significantly less than that observed for the power law experiments reported in [14], [15] and suggests that the Herschel–Bulkley model is a reasonable approximation for the experimental fluid.

The computationally predicted profiles (in conventional wall units based on the mean wall viscosity) are presented in **Figure 11**. This shows good general agreement in terms of shape and magnitude when compared to the experimentally measured profile. All profiles lie slightly above the low Reynolds number Newtonian profile, indicating that the flow is less well developed than that of a Newtonian fluid at similar Reynolds numbers or that there is a fundamentally different turbulent structure in the case of a yield stress fluid. Note that the CFD profiles do not bracket the experimental profile, despite bracketing the Re_g of the experiment. Both lie slightly above, suggesting that there may also be a difference between the flow of a ‘pure’ Herschel–Bulkley fluid (as approximated in the simulations) and the flow of the model fluid used in the experiments. This is not surprising given that the rheology is a curve fit obtained over a limited range of shear rates. Nevertheless, these results are encouraging and suggest that DNS is able to provide reliable predictions of the turbulent flow of shear thinning fluids provided an appropriate choice of rheological model is made.

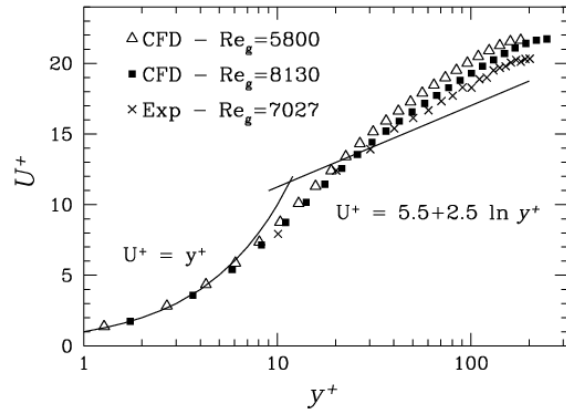


Figure 11: Mean velocity profile in conventional (Newtonian) wall units for a Herschel–Bulkley fluid: comparison of CFD results at $Re_g=5800$ (Δ), $Re_g=8130$ (\blacksquare) and experimental results at $Re_g=7027$ (\times).

The CFD results predict that this flow is also transitional, with slug/puff type behaviour predicted for both Reynolds numbers (not shown). Turbulence intensities and Reynolds stresses follow the same trend as the results for the power law fluids.

The structures and general appearance of the near wall structures are similar to power law fluids and suggest that a small yield stress does not modify the flow significantly. Additional simulations for different flow indices and for a wider range of yield stresses need to be undertaken to more fully explore this issue.

SUMMARY OF RESULTS

The applicability of Clapp’s scaling and log law for power law fluids is backed up by the CFD results for power law fluids. The parameters used by Clapp ($A=3.8$, $B=2.78$) possibly need to be modified to collapse to the generally accepted values for Newtonian turbulence. The results also suggest that as the power law index (n) is decreased, and the deviation from Newtonian rheology increases, the value of Re_g at which transition occurs will also increase. The friction factors predicted by the simulations are 10–15% higher than the Dodge and Metzner [7] correlations obtained from experiment. However, it is not clear if elastic or elongational effects are influencing the results of [7], and thus if the reduction in friction factor there is due purely to shear thinning behaviour or other effects. The simulation results here conclusively show that a reduction in the friction factor results for shear thinning, power law fluids, and thus suggests that at least some of the reduction observed in [7] is due to this alone.

It appears that pipe flow of power law fluids make the transition to turbulence via intermittency and turbulent events like the slugs and puffs observed in Newtonian flow. Although the results are not conclusive because of the insufficient domain length of the simulations, they are believed to be qualitatively correct. These unsteady structures may potentially be able to resuspend small settling particles in particle-laden flows, allowing the transitional regime to be possible for suspension transport in power-law carrier fluids.

Simulations of a Herschel–Bulkley fluid were in reasonable agreement between with Ultrez 10 experimental results. They showed similar behaviour to the power law results, with log-law profiles that lay above the Newtonian profile (suggesting undeveloped flow) and

velocity fluctuations with similar behaviour. Like the power law results, the flow had some suggestion of being transitional, even at a generalised Reynolds number of 8130.

Difficulties encountered in experimentation as a result of using polymer solutions to approximate idealised rheologies can lead to problems of interpretation and understanding. The application of DNS to flows of non-Newtonian fluids with certainty of the rheology being studied has the potential to enable the effect of different rheological parameters to be correctly quantified and understood. This is possibly the greatest contribution that DNS can bring to the study of flows of non-Newtonian fluids. However, given the difficulty in approximating a measured rheology over a very wide range of shear rates using any of the simple generalised Newtonian rheology models, it appears likely that obtaining accurate results of turbulent flow of real non-Newtonian fluids using DNS will remain a difficult task.

ACKNOWLEDGMENTS

The authors gratefully acknowledge the support of AMIRA, BHP–Billiton, De Beers, Rio Tinto, WMC Resources Limited and Warman International (via AMIRA project P599) for partial sponsorship of the work described in this paper.

REFERENCES

- [1] A.N. BERIS, C.D. DIMITROPOULOS, Pseudospectral simulation of turbulent viscoelastic channel flow, *Comput. Methods Appl. Mech. Eng.*, **180**, 365–392 (1999)
- [2] H. M. BLACKBURN, ‘LES of turbulent channel flow using spectral elements’. In: *13th A/Asian Fluid Mech. Conf.* (Melbourne, 1998)
- [3] R. M. CLAPP, ‘Turbulent heat transfer in pseudoplastic non-Newtonian fluids’. In: *Int. Dev. Heat Transfer part III*, (New York, 1961)
- [4] E. DE ANGELIS, C. M. CASCIOLA, R. PIVA, DNS of wall turbulence: dilute polymers and self-sustaining mechanisms, *Computers & Fluids*, **31**, 495–507 (2002)
- [5] R. G. DEISLER, Investigation of turbulent flow and heat transfer in smooth tubes, including the effects of variable fluid properties, *Trans. A.S.M.E.* **73**, 101–107 (1951)
- [6] J. M. J. DEN TOONDER, F. T. M. NIEUWSTADT, Reynolds number effects in a turbulent pipe flow for low to moderate Re , *Phys. Fluids* **9** (11), 3398–3409 (1997)
- [7] D.W. DODGE and A.B. METZNER, Turbulent flow of non-Newtonian systems, *A.I.Ch.E.J.* **5**, 189–204 (1959)
- [8] M. P. ESCUDIER, F. PRESTI, Pipe flow of a thixotropic liquid, *J. Non-Newtonian Fluid. Mech.* **62**, 291–306 (1996)
- [9] M. P. ESCUDIER, F. PRESTI, S. SMITH, Drag reduction in the turbulent pipe flow of polymers, *J. Non-Newtonian Fluid Mech.* **81**, 197–213 (1999)
- [10] G. E. KARNIADAKIS, Spectral element–Fourier methods for incompressible turbulent flows, *Comp. Meth. Appl. Mech. Eng.* **80**, 367–380 (1990)
- [11] G. E. KARNIADAKIS, S. A. ORSZAG, V. YAKHOT, ‘Renormalization Group theory simulation of transitional and turbulent flow over a backward-facing step’. In: *Large Eddy Simulation of Complex Engineering and Geophysical Flows*, ed. by Galerpin and Orszag (CUP, 1993) pp. 159–177
- [12] M. R. MALIN, Turbulent pipe flow of power-law fluids, *Int. Comm. Heat Mass Transfer* **24**, 977–988 (1997)
- [13] F. T. PINHO, J. H. WHITELOW, Flow of non-Newtonian fluids in a pipe, *J. Non-Newtonian Fluid Mech.* **34**, 129–144 (1990)
- [14] M. RUDMAN, H. M. BLACKBURN, L. J. W. GRAHAM, L. PULLUM, ‘Weakly turbulent pipe flow of a power law fluid’. In: *14th A/Asian Fluid Mech. Conf.* (Adelaide, 2001)
- [15] M. RUDMAN, L. J. W. GRAHAM, H. M. BLACKBURN, L. PULLUM, ‘Non-Newtonian turbulent and transitional pipe flow’. In: *Hydrotransport 15*. (Banff, 2002)
- [16] M. RUDMAN, H. M. BLACKBURN, ‘Large eddy simulation of turbulent pipe flow’. In: *2nd Int. Conf. on CFD in the Minerals and Process Ind.* (Melbourne, 1999)
- [17] S. SCHMIDT, D. M. MCIVER, H. M. BLACKBURN, M. RUDMAN, G. J. NATHAN, ‘Spectral element based simulation of turbulent pipe flow’. In: *14th A/Asian Fluid Mech. Conf.* (Adelaide, 2001)
- [18] A. V. SHENOY and D. R. SAINI, A new velocity profile model for turbulent pipe-flow of power-law fluids, *Can. J. Chem. Eng.* **60**, 694–696 (1982)
- [19] R. SURESKUMAR, A. N. BERIS, A. H. HANDLER, Direct numerical simulation of the turbulent channel flow of a polymer solution, *Phys. Fluids* **9**, 743–755 (1997)